

Liquid Phase Epitaxy growth and luminescence of Terbium-doped $\text{Gd}_3\text{Ga}_5\text{O}_{12}$ crystalline layers

Amandine Baillard^{1,*}, Paul-Antoine Douissard², Pavel Loiko¹, Laura Wollesen², Thierry Martin², Eric Mathieu², Eric Ziegler², Gurvan Brasse¹, and Patrice Camy¹

¹Centre de Recherche sur les Ions, les Matériaux et la Photonique (CIMAP), UMR 6252 CEA-CNRS-ENSICAEN, Université de Caen Normandie, 6 Boulevard Maréchal Juin, 14050 Caen, France

²European Synchrotron Radiation Facility (ESRF), 71 Avenue des Martyrs, 38043 Grenoble, France

Abstract. Tb^{3+} -doped single-crystalline $\text{Gd}_3\text{Ga}_5\text{O}_{12}$ layers are grown by Liquid Phase Epitaxy on (111)-oriented undoped substrates, and their structure, composition, morphology and photo- and radioluminescence are studied. Layers doped with 6 at.% Tb^{3+} with a thickness up to 20 μm appear promising for single crystal film scintillators with a sub- μm spatial resolution and waveguide lasers as they exhibit good quality, uniform distribution of Tb^{3+} ions, optimized light output ($\sim 50\%$ of that for $\text{Ce}:\text{YAG}$), weak concentration quenching of luminescence and low afterglow for a 15 bit dynamic range.

1 Introduction

Rare-earth (RE^{3+}) doped single-crystalline layers grown by Liquid Phase Epitaxy (LPE) on oriented bulk undoped substrates are promising for the development of crystalline film phosphors, quantum optics devices, laser waveguides [1] and single crystal film (SCF) scintillators [2]. The latter are used for sub- μm resolution X-ray imaging, allowing non-destructive 3D imaging in applications such as topography, micrography and holography [3]. Trivalent terbium ions (Tb^{3+}) are attractive because of their visible emissions (with the most intense one falling in the green spectral range according to the $^5\text{D}_4 \rightarrow ^7\text{F}_5$ 4f electronic transition). Green Tb-lasers are known [4]. Recently, Tb^{3+} -doped Lu_2SiO_5 SCF scintillators were developed giving improved results in terms of spatial resolution and efficiency [5].

In this work, we report on the Liquid Phase Epitaxy growth, photo- and radioluminescence study of Tb^{3+} -doped $\text{Gd}_3\text{Ga}_5\text{O}_{12}$ (Tb:GGG) SCFs, with the goal of developing new materials for visible waveguide lasers and scintillators with high efficiency for X-ray imaging applications with sub- μm spatial resolution.

2 LPE growth

The terbium doped gadolinium gallium garnet $\text{Gd}_3\text{Ga}_5\text{O}_{12}$ (GGG) films were grown by Liquid Phase Epitaxy on (111)-oriented undoped polished GGG substrates having a diameter of 1 inch and a r.m.s. surface roughness $< 10 \text{ \AA}$. The starting powders for the solution were Gd_2O_3 , Ga_2O_3 , Tb_4O_7 , B_2O_3 and PbO . The initial concentration of Tb^{3+} was in the range of 2 – 10 at.% (with respect to Gd^{3+}). The solution was first homogenized at 1100°C for several hours and then stabilized at the growth temperature

($1010 - 1028^\circ\text{C}$, in the supersaturation domain). To crystallize the cubic garnet phase, an excess of Ga was introduced. The isothermal LPE dipping technique was used. The growth duration was 10 min and the uniform layer thickness was 5 to 12 μm .

The structure (cubic, sp. gr. $Ia\bar{3}d$) and phase purity of the Tb:GGG layers were confirmed by X-ray diffraction. The lattice mismatch was studied by analysing the higher order reflection (888), Fig. 1(a). Tb^{3+} ions substitute for Gd^{3+} ones (ionic radii: $R_{\text{Tb}} = 1.04 \text{ \AA}$ and $R_{\text{Gd}} = 1.053 \text{ \AA}$, for VIII-fold coordination [7]) in dodecahedral (D_2) sites of the GGG lattice leading to a decrease of the lattice parameter of the layer, Fig. 1(b). The composition of the layers was studied by Electron Microprobe Analysis indicating a good homogeneity of Tb concentrations and a close to unity segregation coefficient.

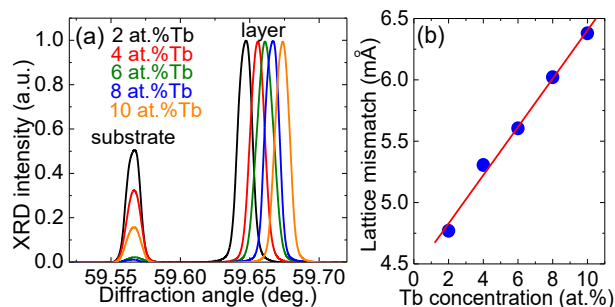


Fig. 1. Influence of the Tb concentration on the lattice mismatch between the GGG substrate and the Tb:GGG layers: (a) (ω , 2θ) scans at the (888) reflection; (b) Linear relation between the lattice mismatch and the Tb concentration.

The as-grown upper face of the Tb:GGG epitaxy was analysed with Atomic Force Microscopy (AFM), showing low surface roughness of $\sim 0.5 \text{ nm}$ over a $50 \times 50 \mu\text{m}^2$ area, Fig. 2(a). The Tb^{3+} ions are uniformly distributed in the

* Corresponding author: amandine.baillard@ensicaen.fr

layer with no diffusion into the substrate, as evidenced by the μ -luminescence mapping, cf. Fig. 2(b), monitoring the green luminescence from Tb^{3+} ions.

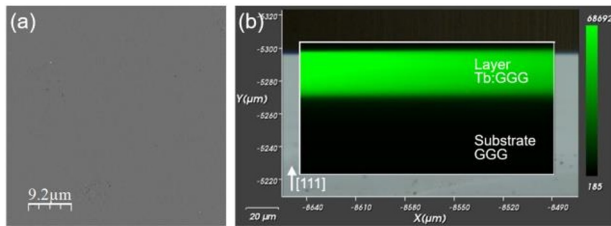


Fig. 2. (a) Top view by AFM of a $50 \times 50 \mu\text{m}^2$ region on the upper face of an as-grown Tb:GGG layer; (b) Micro-luminescence mapping across an end-facet of a 8 at.% Tb:GGG epitaxy, $\lambda_{\text{exc}} = 488 \text{ nm}$, $\lambda_{\text{lum}} = 544 \text{ nm}$.

3 Luminescence properties

The luminescence excitation spectrum of Tb^{3+} ions in the Tb:GGG epitaxial layer is shown in Fig. 3(a), monitoring the green emission at 543 nm. The transition in absorption ${}^7\text{F}_6 \rightarrow {}^5\text{D}_4$ corresponds to a distinct band falling in the blue spectral range with a maximum at 488 nm and in the UV, the bands are due to transitions to overlapping ${}^5\text{D}_1$, ${}^5\text{G}_1$, ${}^5\text{L}_1$ 4f multiplets. Tb^{3+} ions feature multi-colour emissions in the visible from the metastable state ${}^5\text{D}_4$ to a group of lower-lying ${}^7\text{F}_J$ levels ($J = 0 - 6$, ${}^7\text{F}_6$ is the ground-state), Fig. 3(b).

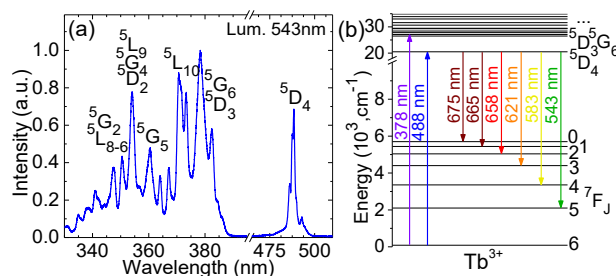


Fig. 3. (a) Luminescence excitation spectrum of Tb^{3+} ions in the Tb:GGG epitaxial layer, $\lambda_{\text{lum}} = 543 \text{ nm}$; (b) Energy-level scheme of Tb^{3+} ions.

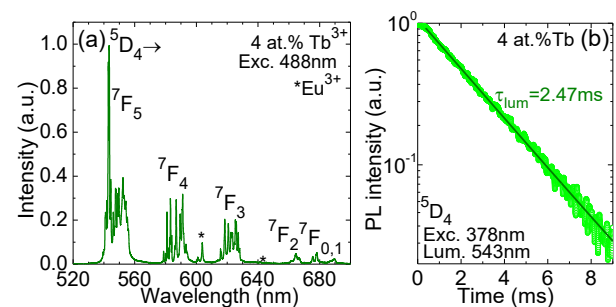


Fig. 4. Photoluminescence properties of 4 at.% Tb:GGG layers: (a) Luminescence spectrum, $\lambda_{\text{exc}} = 488 \text{ nm}$; (b) Luminescence decay curve from the emitting ${}^5\text{D}_4$ Tb^{3+} state, $\lambda_{\text{exc}} = 378 \text{ nm}$, $\lambda_{\text{lum}} = 543 \text{ nm}$ (symbols – experim. data, line – exponential fit).

The ${}^5\text{D}_4 \rightarrow {}^7\text{F}_5$ Tb^{3+} transition is responsible for the most intense emission in the green between 540 – 556 nm, see Fig. 4(a), showing the photoluminescence spectrum. The weak background emissions marked by asterisks are

assigned to impurity Eu^{3+} ions in the GGG substrate. The luminescence decay from the ${}^5\text{D}_4$ metastable state of Tb^{3+} ions was studied, see Fig. 4(b). The decay is nearly single-exponential and the measured luminescence lifetimes τ_{lum} are 2.62 ms (2 at.% Tb), 2.47 ms (4 at.% Tb) and 2.37 ms (6 at.% Tb), representing weak concentration-quenching.

The light output was measured with an X-ray generator using a Copper anode. We noticed an improvement in the light output as the Tb concentration in the layer increased to 6 at.%. Above this doping level, its value stabilized at the maximum value of $\sim 50 - 52\%$. The radioluminescence spectra of the layers were recorded at the X-ray energy of 8 keV. The Tb:GGG layer emission spectrum contained characteristic bands assigned to transitions of Tb^{3+} ions from the short-living ${}^5\text{D}_3$ and metastable ${}^5\text{D}_4$ states to the group of lower-lying ${}^7\text{F}_J$ manifolds. The afterglow of the SCF was studied. After 100 ms, the emission intensity drops down to 4×10^{-5} , corresponding to a dynamic range of more than 14 bit.

4 Conclusion

The growth of Tb^{3+} -doped GGG single-crystalline layers on undoped GGG substrates by LPE is demonstrated. High quality layers up to $20 \mu\text{m}$ thickness can be obtained. The Tb^{3+} dopant is uniformly integrated in the layers. The concentration of 6 at.% Tb in the melt yields layers with optimized light output. The luminescence in the green part of the visible spectrum due to the 4f electronic transitions of Tb^{3+} ions fits well with back-illuminated, interlined CCD cameras and recent scientific CMOS cameras. The conversion efficiency of the Tb:GGG film is relatively low (only 50% of that for Ce:YAG), but the afterglow is absent from the films for a 15 bit dynamic range. Further purification of the GGG substrates (*i.e.*, removal of the Eu^{3+} impurity) is essential for applications.

References

1. W. Bolaños, G. Brasse, F. Starecki, A. Braud, J.-L. Doualan, R. Moncorgé, P. Camy, *Opt. Lett.* **39**, 4450 (2014).
2. T. Martin, P.-A. Douissard, M. Couchaud, A. Cecilia, T. Baumbach, K. Dupre, A. Rack, *IEEE Trans. Nucl. Sci.* **56**, 1412 (2009).
3. A. Koch, C. Raven, P. Spanne, A. Snigirev, *J. Opt. Soc. Am. A* **15**, 1940 (1998).
4. P. W. Metz, D.-T. Marzahl, A. Majid, C. Kränkel, G. Huber, *Laser Photon. Rev.* **10**, 335 (2016).
5. T. Martin, A. Koch, *J. Synchrotron Radiat.* **13**, 180 (2006).
6. P.-A. Douissard, A. Cecilia, T. Martin, V. Chevalier, M. Couchaud, T. Baumbach, K. Dupré, M. Kühbacher, A. Rack, *J. Synchrotron Radiat.* **17**, 571 (2010).
7. R. D. Shannon, *Acta Crystallogr. A* **32**, 751 (1976).